



Convention on the Law of the Sea (UNCLOS) for an extended continental shelf (Gardner et al., 2006a). The bathymetry and 12-kHz acoustic backscatter of the West Mariana Ridge, from 13°20'N to 21°00'N and from the crest of the Ridge to the western margin where it merges with the Parece Vela Basin in water depths of almost 5000 m has now been mapped almost in its entirety (Gardner, 2006, 2008). The new data reveal a series of isolated or coalesced volcanic seamounts, several of which rise along the West Mariana Ridge crest almost to the sea

surface and an extensive volcanic apron that has buried much of the western flank of the volcanic edifice. In addition, a remarkable series of well-developed (implying relatively young to active) channel systems were found that incise the volcanic apron on the western flank of the West Mariana Ridge.

The new MBES surveys are the first high-resolution bathymetric maps of this large area (>184,000 km<sup>2</sup>) of seafloor in the western Pacific. Stern and Smoot (1998) published 200-m contour maps and gridded digital terrain models

(DTMs) of unknown pixel resolution of the Mariana forearc, but their data do not extend far enough to the west to adjoin the new MBES data. The highest resolution bathymetry of this region available prior to the MBES surveys is the ~1.8 km/pixel-resolution satellite altimetry (Smith and Sandwell, 1997, 2004) (Fig. 2A). At this rather coarse resolution, only the gross morphology of the seafloor geomorphology is resolved. Japan has conducted MBES mapping to the west, north, and, to some extent, to the east of the West Mariana Ridge, but not

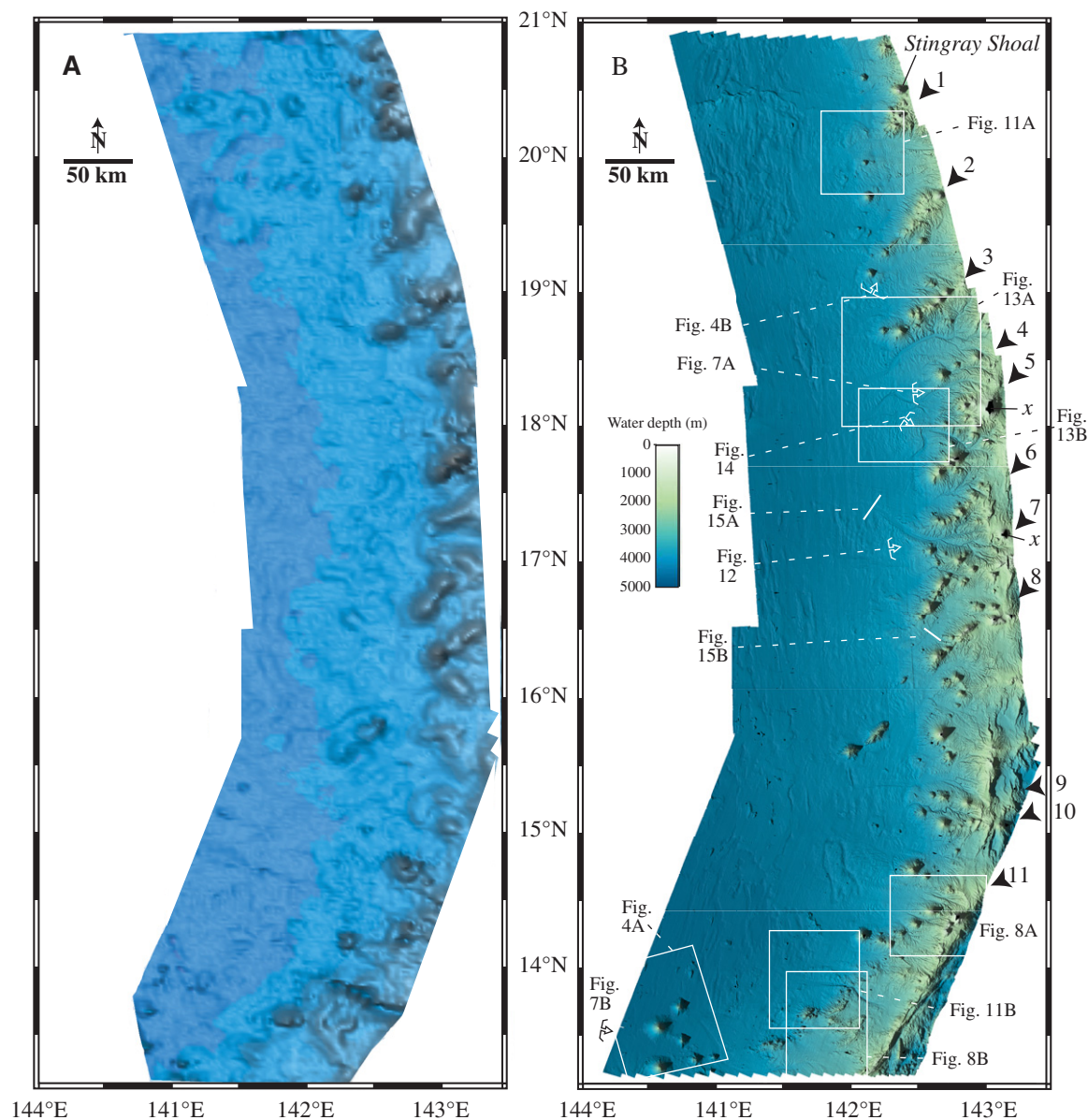


**Figure 2.** Comparison of (A) Smith and Sandwell (1997) satellite altimetry bathymetry of mapped area and the (B) new multibeam bathymetry. Location for subsequent figures shown by white squares and white arrowheads with white dashed leaders. Black numbered arrowheads point to cross-chain volcanoes. Solid white line is location of high-resolution subbottom profiler line.

of the Ridge proper, although their data are presently not publicly available. The 100-m/pixel resolution of the new MBES bathymetry grid provides a much more detailed view of the West Mariana Ridge that resolves mesoscale (a few hundred meters) features (Fig. 2B). The focus of this paper is to describe the geomorphology of the Ridge from the newly acquired MBES data from its crest to its western flank and propose processes that the geomorphology suggests have modified this margin.

## Background

The West Mariana Ridge is the southwestern component of the Izu-Bonin-Mariana arc system. The arc system is nearly 3000 km long and resides on the eastern edge of the Philippine Sea plate. Studies of the Mariana arc system suggest that the West Mariana Ridge is a remnant arc (Karig, 1971, 1972) produced by Miocene backarc spreading in the Mariana Trough that is suspected to have separated from the West Mariana Ridge from the volcanically active Mariana arc from 8 to 6 Ma (see discussions by Fryer, 1995, 1996; Stern et al., 2003). Volcanism along the West Mariana Ridge is thought to have ceased ~7 Ma (Stern et al., 2003), and since that time the Ridge is thought to have subsided (Karig and Glassley, 1970), presumably following the subsidence curve of the Philippine Sea plate (Park et al., 1990) upon which the Ridge was constructed. There has been very little sampling of the West Mariana Ridge; Deep Sea Drilling Project (DSDP) Site 451 (Fig. 1) recovered fragments of andesite and basaltic andesite in the bottom of the hole on the summit of the Ridge (Kroenke, et al., 1981), and Karig and Glassley (1970) report dacite pumice from dredge hauls from the eastern scarp of the Ridge. These appear to be the only samples of the volcanic rocks from the West Mariana Ridge other than ubiquitous ash described from 21 piston cores and from the upper sections of four DSDP drill sites in the area (Fig. 1).

## MBES Systems and Data Processing

The new MBES mapping used a 12-kHz Kongsberg Simrad EM121A multibeam system that generates 121  $1^\circ \times 1^\circ$  receive apertures to provide a continuous  $120^\circ$  swath of soundings. Refraction of the acoustic pulse in the water column was modeled by calculated sound-speed profiles from 263 expendable bathythermograph casts, nine expendable sound-velocity casts, and three CTD casts throughout the two months of mapping. Sound speed at the transducer was continuously monitored using an Applied Microsystems Smart SV&T sound-

velocity sensor. Instantaneous ship heave and pitch and roll were recorded with an Applanix POS/MV model 320 motion-reference unit, and heading was provided by a Sperry model 39 gyro. The EM121A can compensate for pitch and roll but not yaw. The Applanix POS/MV was interfaced with two Trimble Force 5 GRAM-S global positioning system (GPS) receivers using NavCom Defense Electronics Starfire SF2050R wide-area differential GPS that provide position fixes with an accuracy of  $<\pm 0.5$  m. All horizontal positions are georeferenced to the WGS84 ellipsoid, and vertical referencing is to instantaneous sea level. Seventy cross-line intersections provide an evaluation of the precision of both the beam ray tracing and the depth resolution of the EM121A MBES. The mean depth error from the cross-line analyses ( $n = 16,772,630$  soundings) is 0.07% for water depths from 2000 to 4900 m.

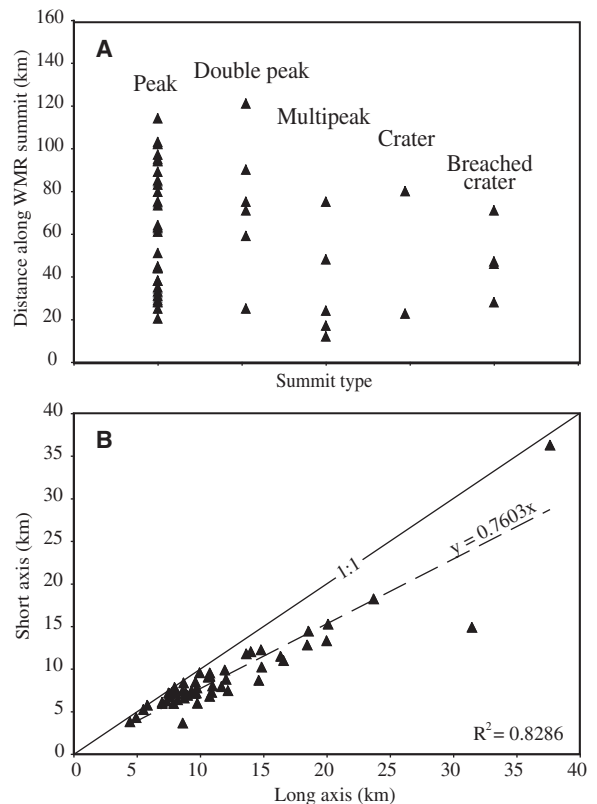
The raw multibeam bathymetry and acoustic backscatter data were processed aboard ship using the University of New Brunswick's *SwathEd* software suite (J. Hughes Clarke, 1996, personal commun.), version 200708096. After the bathymetry was edited, the valid soundings were gridded into a digital terrain model (DTM). The co-registered, beam time-series, acoustic backscatter was assembled and gridded into a backscatter mosaic using

the University of New Hampshire—developed *Geocoder* software (Fonseca and Calder, 2005; Fonseca and Mayer, 2007).

## GENERAL GEOMORPHOLOGY

The West Mariana Ridge separates two basins—the Mariana Trough, a  $>3000$ -m-deep, actively spreading, backarc basin to the east and the ~5000-m-deep Parece Vela Basin to the west (Fig. 1). The overall morphology of the West Mariana Ridge is a gently arcuate SSE- (at the north end) to SSW-trending (at the south end) edifice of single and coalesced submarine volcanic peaks (the term *volcano* is used interchangeably with *volcanic peak*) along the Ridge crest and to the immediate west of the crest. The West Mariana Ridge has a steep ( $10^\circ$  to  $14^\circ$ ) east-facing flank thought to be a fault scarp that resulted from the splitting of the active arc by backarc spreading in the Mariana Trough that began ~7 Ma (Hussong and Uyeda, 1981; Fryer, 1996; Stern et al., 2003). The west-facing flank has gentle slopes ( $3^\circ$  to  $4^\circ$ ) and is blanketed by an apron of volcanoclastic sediments. Although Karig (1971) suggests the west-facing flank of West Mariana Ridge is also a fault scarp, later studies (e.g., Hussong and Uyeda, 1981; Fryer, 1996) do not support this interpretation. However, the western slope of the Ridge must have

**Figure 3.** Plots of (A) summit type versus distance from north to south between volcanoes projected to a line along the crest of the West Mariana Ridge (WMR) and (B) individual long basal axis versus short basal axis.



originally formed by rifting to open the Parece Vela Basin ~30 Ma but has since been extensively modified by subsequent arc volcanism and sedimentation (R.J. Stern, 2009, personal commun.). The crest of the West Mariana Ridge is intersected by a prominent series of cross-chain volcanoes (numbered black arrowheads in Fig. 2B) that trend a fairly consistent ~60° to the trend of the crest of the Ridge. None of the volcanoes of the crest or the cross chains presently rise above sea level, although a few come close to sea level. The main volcanic ridge including the cross-chain volcanoes cover an area of ~52,000 km<sup>2</sup>. The sediment apron that covers the western flank of the West Mariana Ridge covers ~73,000 km<sup>2</sup> and is composed of sediments that were transported from the volcanic edifice by large, relatively unconstrained downslope sediment failures as well as through a series of well-defined submarine channels. The basement topography beneath the Parece Vela Basin west of the sediment apron is covered by a relatively thin veneer of ash-rich pelagic clay (Fisher et al., 1971; Kroenke et al., 1981).

The northern one-third of the MBES survey did not completely map the summit of the West Mariana Ridge, although the southern two-thirds of the survey mapped the entire crest. In all, 82 individual volcanic peaks were mapped, and, of those, 25 peaks have summits with water depths of less than 1000 m, and 11 summits have depths less than 500 m. Five of the volcanoes have summit craters, and two are guyots; the remaining 75 seamounts are peaked volcanoes (Fig. 3A). The flank slopes of individual volcanoes range from 12° to 34° with a mean of ~21° ( $\sigma = 5^\circ$ ). The West Mariana Ridge slopes are steeper than those tabulated by Jordan et al. (1983), who calculated average slopes of 15°. The most striking statistic of the individual seamounts is their basal asymmetry; they have a short axis ~75% of the length of the long axis (Fig. 3B). The long axes of cross-chain volcanoes tend to parallel the chain trend, but the summit volcanoes have no particular preferred trend of the long axis. A rift in a volcanic peak is commonly seen to parallel its long axis (Fig. 4A), and an elongated dike-like feature is often found in the space between adjacent volcanoes within the cross chains (Fig. 4B).

There is no latitudinal trend to the summit depths, although the largest concentration of deep summits occurs on individual cross-chain seamounts in the southernmost part of the mapped area (Figs. 5 and 6A). There is also no apparent tendency of summit depth (Fig. 6B) or volcano volume (Fig. 6C) and no trend in flank slope with latitude or basal water depth. However, there is a rough normal distribution of the distance along trend from the summit of West

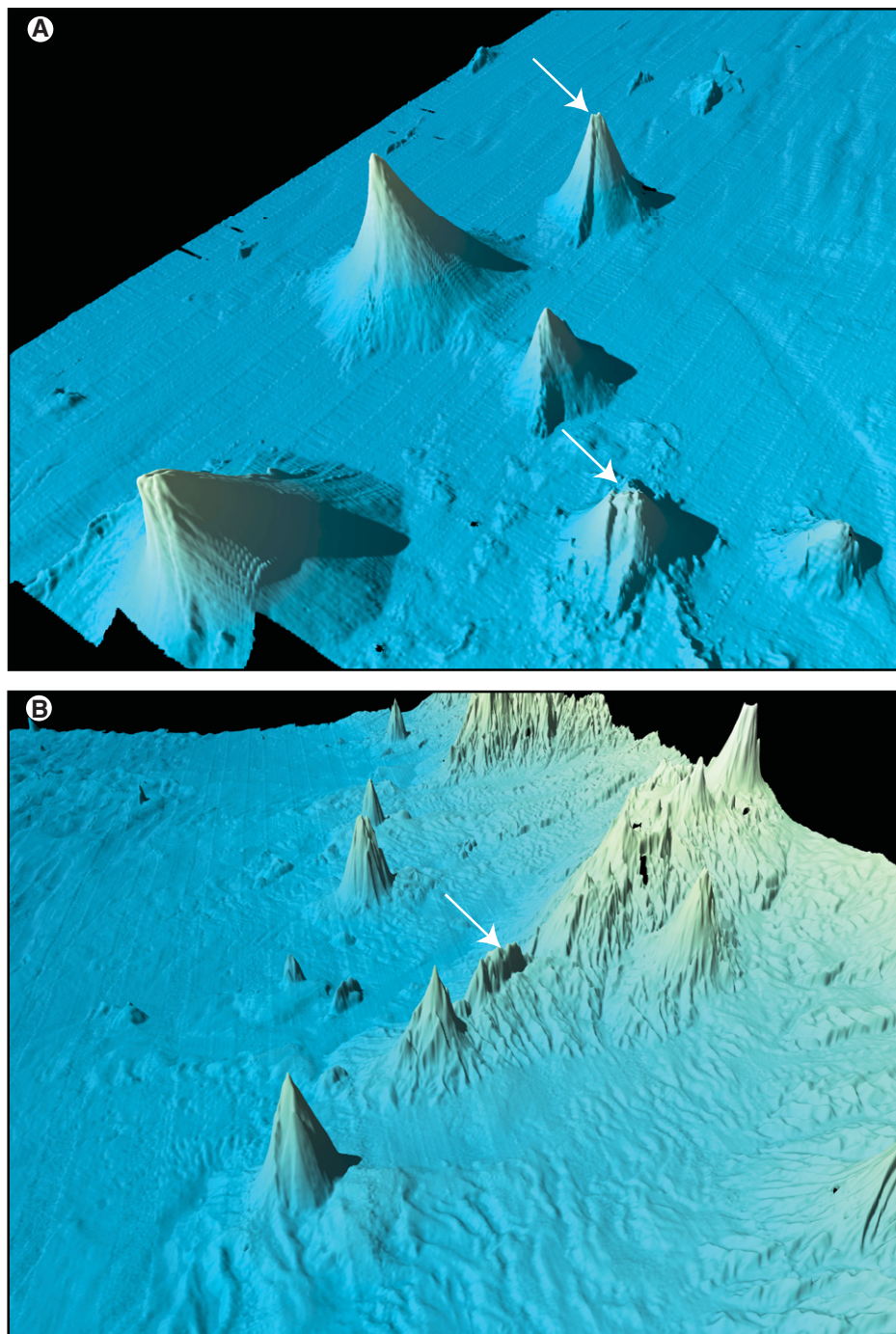


**Figure 4.** Perspective views of individual volcanoes showing examples of rifted peaks (arrows in A) and dike-like feature (arrow in B). Vertical exaggeration = 5×.

Mariana Ridge (Fig. 6D). The shallowest seamounts are Stingray Shoal (Figs. 2 and 6A) with a summit of only 16 m and two unnamed guyots with summits of 7 m and <7 m deep (Fig. 6A). The summits of the two guyots were not completely mapped for fear of running aground.

Cross chains are linear seamount chains that cross the trend of the main volcanic arc at high

angles. Eleven cross chains intersect the West Mariana Ridge and extend as much as 130 km to the SW away from the Ridge (numbered black arrowheads in Fig. 2B). Whether or not the cross chains extend to the east is unknown, although the updated 1-min-resolution, satellite-derived bathymetry of Smith and Sandwell (1997) suggests they may not. The cross chains to the

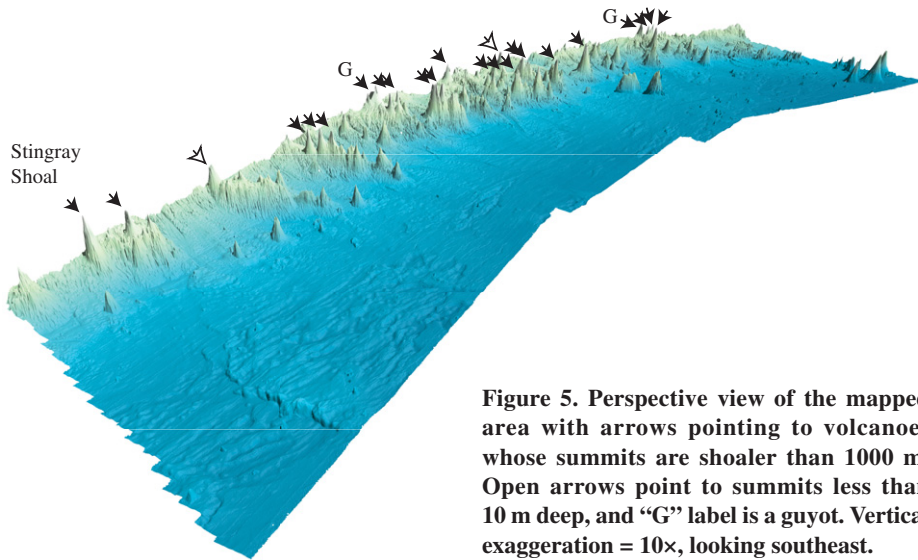


**Figure 5.** Perspective view of the mapped area with arrows pointing to volcanoes whose summits are shallower than 1000 m. Open arrows point to summits less than 10 m deep, and “G” label is a guyot. Vertical exaggeration = 10 $\times$ , looking southeast.

west of West Mariana Ridge are separated from one another along each trend by an average of 46.5 km ( $\pm 17.1\text{ km } 1\sigma$ ). Cross chains are separated farther from one another in the north and become closer spaced in the south. The trends of the cross chains vary in strike from  $033^\circ$  to  $060^\circ$ . The cross chains of the West Mariana Ridge typically are linear in trend and do not show the pronounced curvilinear trend of cross chains of

the Izu-Ogasawara arc to the north (Ishizuka et al., 1998). The cross chains of the West Mariana Ridge have never been dated, or even sampled for that matter, but the Izu-Ogasawara arc cross chains do not show a progression of ages trending toward or away from the main volcanic ridge (Ishizuka et al., 1998).

Fryer et al. (1997) suggest that the cross chains represent a weakness of the crust inher-

ited from strain developed by tectonic activity during forearc, volcanic front, and backarc rifting. They speculate that as the convergent margin evolves, volcanism is directed to these cross-arc rifts.

## EROSION OF VOLCANOES

Statistics of the morphology of individual seamounts, such as summit depth, base depth, flank slope, etc., show no latitudinal or water-depth correlations. However, the preservation of individual volcanoes appears to change from being heavily eroded in the north to less eroded in the south (Fig. 7). Dissection of a volcano's flank is the most obvious evidence of erosion. Most of the northern volcanoes show dissection from their base to typically half way to their summits, and the dissection is generally  $>20\text{ m}$  deep even on their upper flanks. In contrast, the southern volcanoes show little or no dissection on the upper flanks and only minor dissection on their lower flanks. The northern volcanoes also have much larger accumulations of sediment around their bases as compared to the southern volcanoes, again suggesting a younging toward the south.

The lower flanks and bases of the cross-chain volcanoes show significant erosion by channel systems that traverse downslope from the summit region on the east to the Parece Vela Basin to the west (Fig. 8). The channel systems in the

**Figure 6.** (A) Plot of volcano-summit water depth versus latitude. Dashed line at 500-m water depth. Location of Stingray Shoal (arrow) shown on Figure 5. (B) Histogram of volcano summit depths. (C) Histogram of volcano volume (dashed line is normal distribution). (D) Histogram of distance of volcanoes from West Mariana Ridge crest as measured along trend (dashed line is normal distribution).

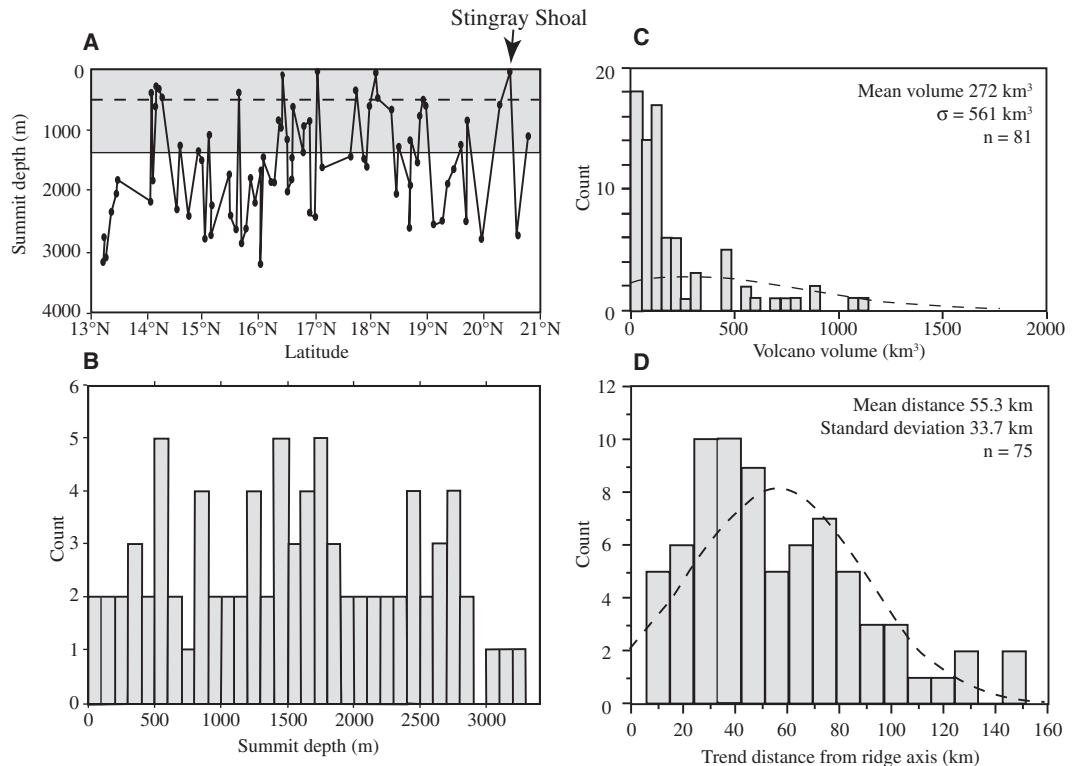
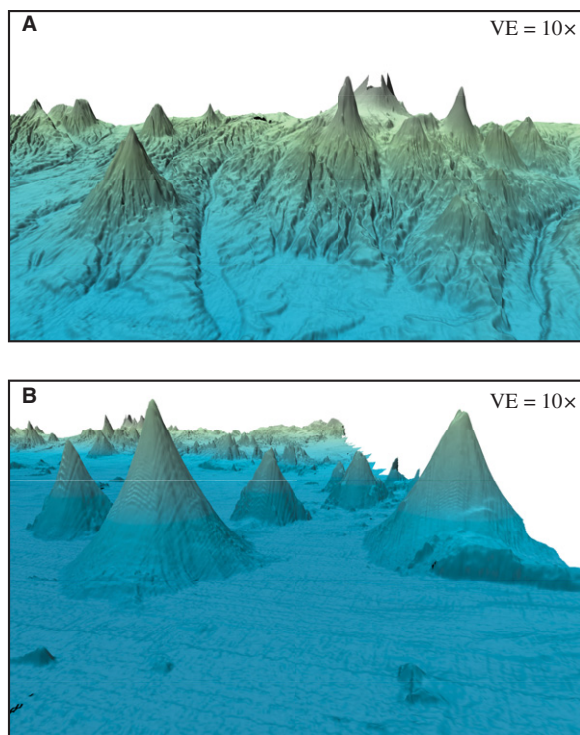


**Figure 7.** Perspective views of examples of flank erosion on volcanoes from the north (A) and south (B). Note the extensive dissection of the flanks in the north compared to the fresh-looking flanks in the south. VE—vertical exaggeration.



north generally have well-defined incised thalwegs within sediment-filled channels, whereas the channels in the south have less pronounced or no thalwegs, suggesting, like the erosion of the volcanoes, that the channel systems in the south are younger than those of the north (Fig. 8A versus 8B).

**SEDIMENT APRONS**

Large, sometimes coalesced, sediment lobes form a huge composite sediment apron along the entire western lower flank of the West Mariana Ridge (Fig. 9). The acoustic-backscatter image shows the high-backscatter response of the dis-

placed sediment (Fig. 9B). Individual sediment lobes appear to be formed by downslope creep of sediment masses, as suggested by the ridge-and-swale surface morphology (Fig. 10) and by the subbottom-reflection character seen in the few seismic profiles from previous cruises. The ridge-and-swale texture is somewhat similar, but much larger in scale, than features described from the flanks of the Mariana active arc by Embley et al. (2006) and interpreted by them as dunes. The ridges of the ridge-and-swale topography of the West Mariana Ridge range from 6 to 60 m high (mean = 17 m) and have wavelengths that range from 0.7 to 3.9 km (mean = 1.8 km). Unfortunately, all the MBES tracklines are oriented 175° to 355°, so the high-resolution subbottom profiler data collected along track during the cruises do not cross the ridge-and-swale topography on a trend that would shed light on the subsurface architecture of these features. However, the few existing seismic records that do trend downslope and across the sediment aprons show a 250- to 300-m-thick section of gently deformed sediments. The apron thins and becomes less deformed to the west, where it eventually merges with the thin pelagic clays of the Parece Vela Basin.

There is evidence that some of the creep lobes are younger than the latest stage of channel erosion, although most of the creep lobes appear to be eroded by adjacent channel systems. More recent creep lobes can be seen where the ridge-and-swale topography of a creep lobe has buried an adjacent channel (white bracket on

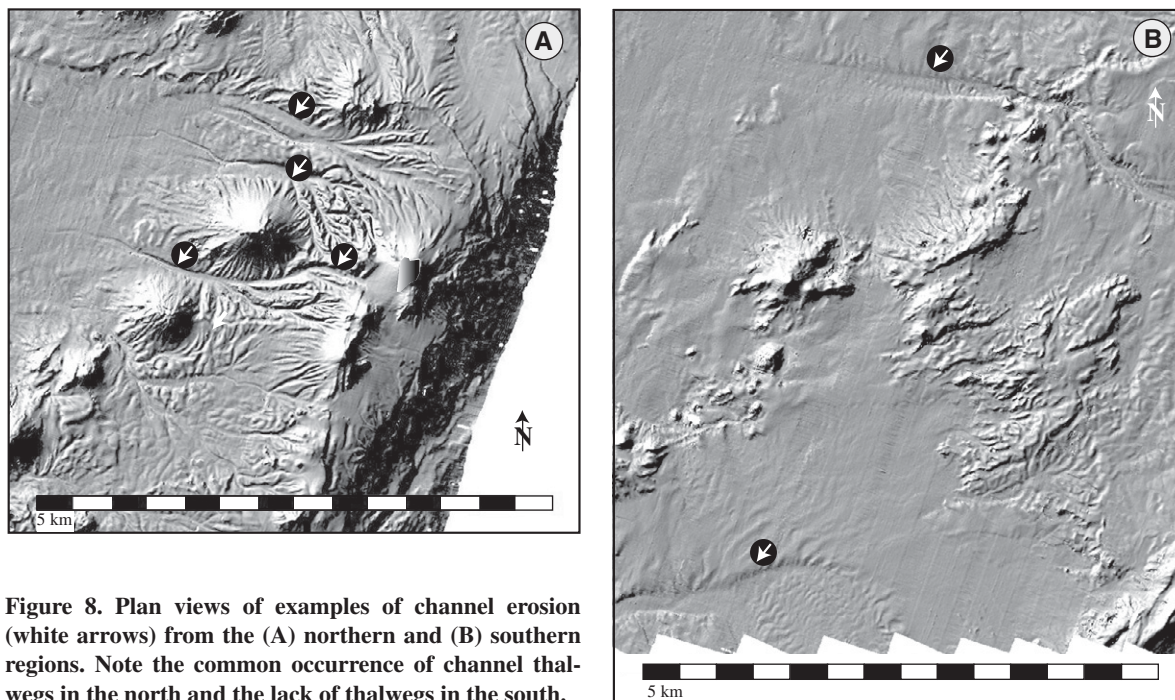


**Figure 8.** Plan views of examples of channel erosion (white arrows) from the (A) northern and (B) southern regions. Note the common occurrence of channel thalwegs in the north and the lack of thalwegs in the south.

**Figure 9. (A) Bathymetry base map with interpretations of volcanic aprons, depositional lobes, and drainage systems. (B) Acoustic backscatter (12 kHz) of mapped area. Yellow line represents western extent of the sediment apron.**

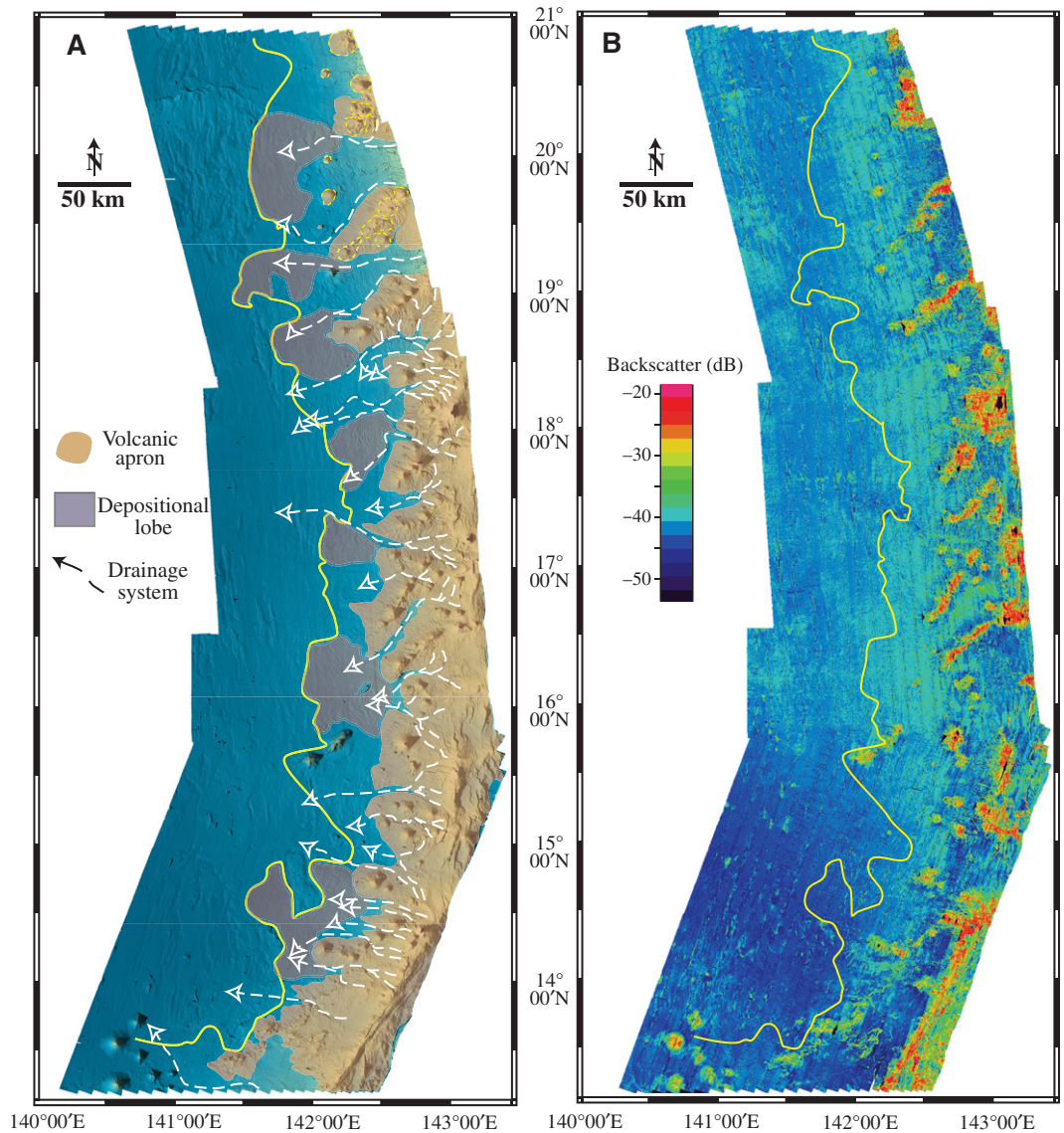


Fig. 11A). However, the ridge-and-swale topography of many of the creep lobes has been incised by later channel erosion (white arrows on Figs. 10 and 11B). Several of the channels have been steered around the higher relief of an individual creep lobe (white arrowhead on Fig. 10), again suggesting the apron deposit existed prior to channel erosion.

#### CHANNEL SYSTEMS

The most surprising discovery from the new bathymetry survey is the large, well-developed submarine channel systems that strike to the west from the summit region of the West Mariana Ridge. Although channel systems have been described from other island-arc systems (e.g., von Huene and Arthur, 1982; Klaus and Taylor, 1991; Embley et al., 2006; among others), all

these occurrences are described from forearc areas of active island arcs with their attendant tectonic processes. In contrast, the submarine channels of the western flank of West Mariana Ridge are found in a remnant arc thought to be presently nontectonic and dormant for the past 7 m.y. (Fryer, 1996; Stern et al., 2003).

The new MBES mapping located 27 main channels along the 740-km length of West Mariana Ridge with the best developed channels in the north and central regions (Fig. 9A). Typically, the channels evolve from a relatively short upper section that is ~5 km long that could be classified as a canyon (Fig. 12). These canyon sections have walls 200 to 300 m high with slopes of >10° and a valley floor generally ~100 m wide at the base. The canyons typically display a dendritic pattern of secondary and tertiary arms that join the main canyon at

a drop-off of several meters to as much as 35 m (Fig. 12). The junctions of the secondary channels with the main channel vary in angle from 90° to less than 20°.

The canyons evolve down slope into broad flat-floored channels that often are incised into the apron sediments (Figs. 10, 11B, and 13), and several of the channels have incised through sections of the volcanic edifice as well (Figs. 8A, 10, and 13). The main channels range in width from 950 to greater than 3000 m, some with well-defined inner-bend terraces (Fig. 13). The channels have incised downward from 50 m to more than 275 m into the volcanic edifices and sediment apron with channel trends that vary from almost straight to ones that have bends in excess of 100°. The channels have a sinuosity index (ratio of channel length to straight-line distance; Leopold et al., 1964) that would classify them

as straight to slightly meandering channels (i.e., sinuosity index  $\sim 1.06$ ). The channel walls typically have slopes of  $5^{\circ}$ – $15^{\circ}$ . Several of the broad channels in the central part of the West Mariana Ridge have a well-defined narrow (75–100 m) thalweg that has entrenched as much as 50 m into previous channel fill, suggesting multiple episodes of channel development.

All of the high-resolution CHIRP profiles (28,674 km of lines in total with a 10-km average line spacing oriented roughly N-S) that cross the channels show a thick, acoustically transparent pelagic sequence on either side of the channel but a complete lack of pelagic sediment within the channel (Fig. 14). The channel sediments are acoustically opaque throughout their reaches with no suggestion of the pelagic sediment that is seen in the immediately adjacent seafloor. Consequently, the channels appear to have been recently active and are not a legacy of when the West Mariana Ridge was an active volcanic arc.

Typical fluvial-like features are found throughout the channels. For example, hummocky and high-backscatter inner-bend areas, inner-bend terraces, channel-wall failures, point bars, incised thalwegs, etc. (Leopold et al., 1964) are found in many of the channels. In addition, the second- and third-order dendritic pattern of the channels is very similar to subaerial fluvial channels. Although the high-resolution bathymetric data are amenable to a detailed statistical analysis of the dendritic networks (e.g., Horton, 1945; Strahler, 1952), work by Kirchner (1993), Masek and Turcotte (1994), and Troutman and Karlinger (1994) suggests the classic geometric parameters are not indicative of any specific mode of formation but rather are attributes of all networks, real or synthetic. Consequently, no attempts were made to measure stream order, channel length, length ratios, etc.

The surprising nature of these submarine channels is not their resemblance to subaerial fluvial channels (comparisons of similarities between subaerial and submarine channels have been made several times; e.g., Flood and Damuth, 1987; Clark et al., 1992; Primez and Flood, 1995; Babonneau et al., 2002; Kolla et al., 2007; among others). The surprise comes from the channels' apparent youthfulness on a feature that supposedly has been quietly subsiding, and thus reducing the overall gradient, for the past 7 m.y.

## DISCUSSION

There are three aspects of the geomorphology of West Mariana Ridge that appear to be directly related to major processes that have modified this landscape after it became sepa-

**Figure 10.** Plan view of an example of ridge-and-swale topography of a creep lobe. Profile X–X' shown on bottom. White open arrowhead shows where a channel has been steered around the creep lobe.

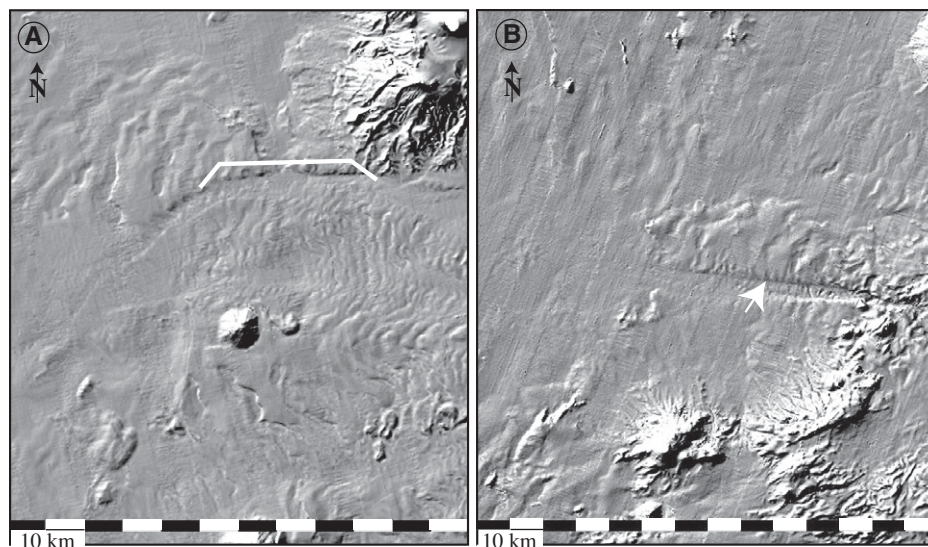
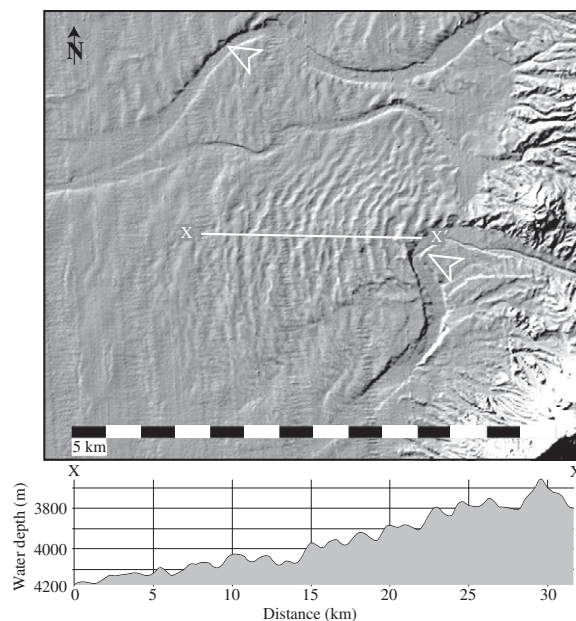


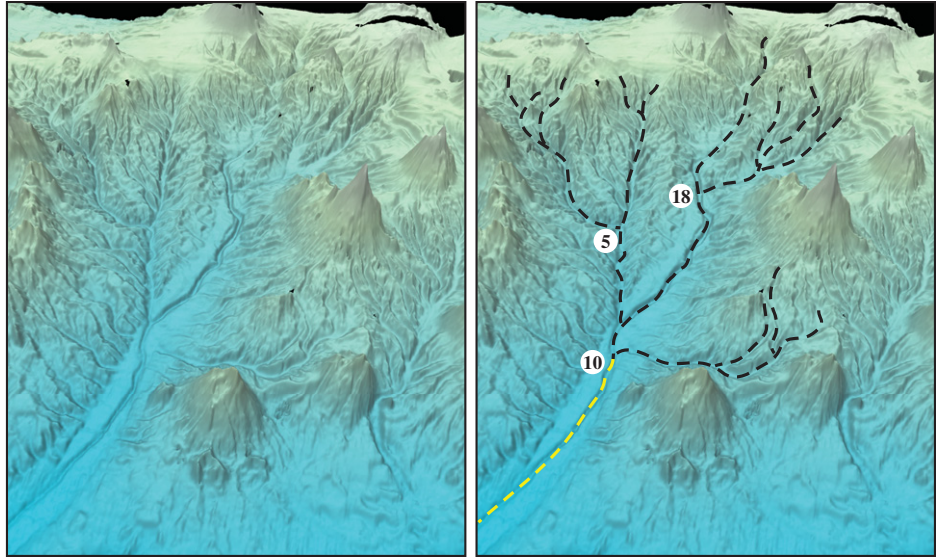
**Figure 11.** Plan views of creep lobes on the flank of the West Mariana Ridge. Large-scale, ridge-and-swale topography on the creep lobes suggests downslope creep. White bracket in (A) is area where a failure has buried the adjacent channel. White arrow in (B) points to example where creep lobes have been eroded by channel erosion.

rated from the Mariana arc. The first aspect is the shallow nature of many of the summits of the crest volcanoes. Almost all of the volcano summits are peaked, rather than cratered or flat topped. Certainly, the two guyots, with summit depths of  $\sim 7$  m, were subaerial volcanoes at one time, and both have been planed off at sea level, as evidenced by their shallow depths. The predominance of peaked volcanoes suggests that either most of the volcanoes were constructed by submarine eruptions or that,

if they were subaerially formed, they subsided beneath effective wave base so rapidly that their tops or flanks were not noticeably eroded. If this distal edge of the Philippine Sea plate has followed the subsidence curve of Park et al. (1990) since volcanic activity on the West Mariana Ridge ceased  $\sim 7$  m.y. ago, then the crest of the Ridge should have subsided  $\sim 1200$  m from its height when active. The rate of subsidence for the first 500 k.y. of new Philippine Sea plate crust decreased from



Figure 12. Perspective view of an example of a canyon and upper channel. Right panel shows interpretation with canyon as black dashed line and channel as yellow dashed line. Numbers represent the height of drop-off of tributary canyon into main canyon. Vertical exaggeration = 5 $\times$ , looking east.



0.5 m/k.y. to 0.2 m/k.y. Twenty-eight peaks are presently at or shallower than 1200-m water depth. If these volcanoes formed at or above sea level, why do they not show signs of flank or summit erosion? There appears to be plenty of time for wave-base erosion to plane off or form a wave-cut terrace on the volcanoes. Why were they not planed off into guyots, or at least

why are there no wave-base terraces on their flanks? What can account for the apparent lack of subsidence, or, if almost all of the volcanoes are submarine in origin, what caused a renewed uplift of the West Mariana Ridge?

The second aspect seen in the geomorphology is the apparent younging of the volcanism from north to south. Evidence from the erosion

on the flanks of the volcanoes, together with the debris surrounding the bases of the volcanoes, suggests that the volcanoes in the northern area of the West Mariana Ridge are older than those in the southern area. Apparently, volcanism was not constant along the length of the Ridge when it was active. However, that said, there are five volcanoes within a relatively small region in

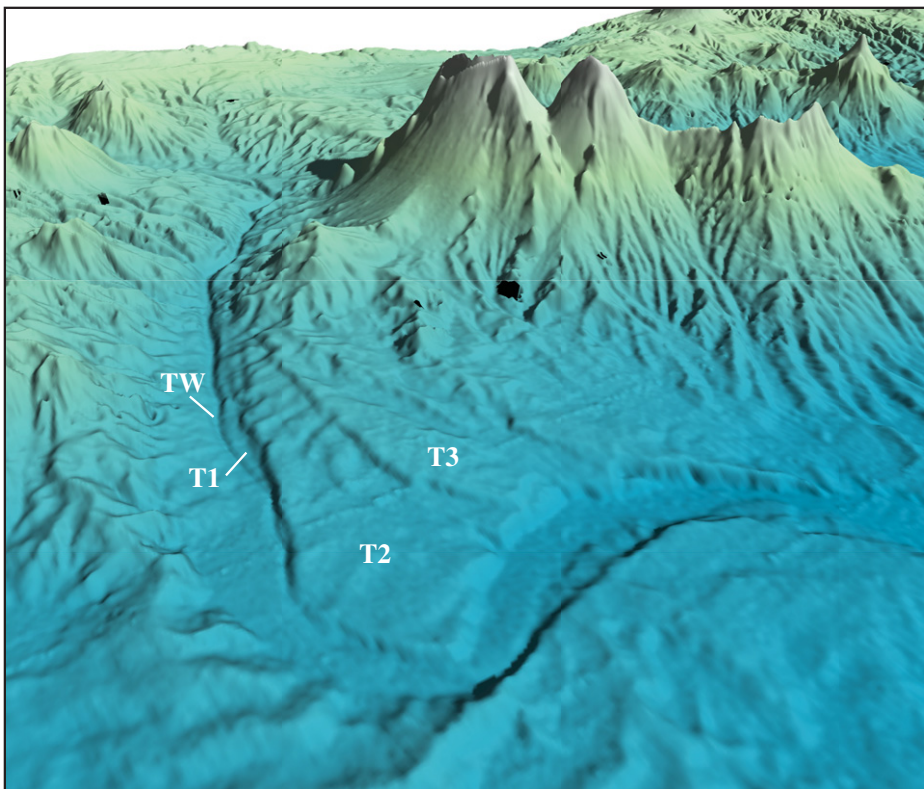
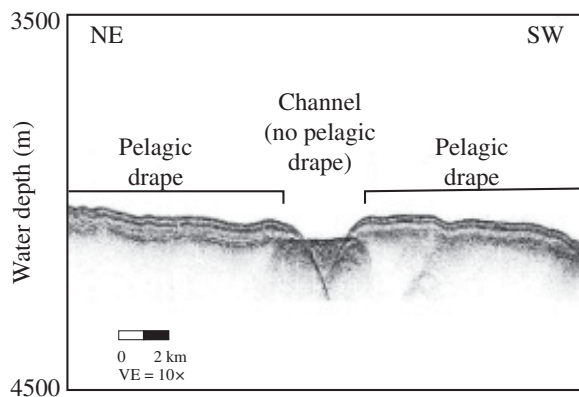


Figure 13. Perspective view of an example of channel with an incised thalweg (TW). This channel system has a perched terrace (T1) and inner-bend terraces (T2 and T3). Vertical exaggeration = 3 $\times$ , looking southeast.

**Figure 14. Typical high-resolution, subbottom profile across a channel. Note the hard reflector and lack of pelagic-like drape on the channel surface compared to the pelagic-like drape on the adjacent seafloor. VE—vertical exaggeration.**



the northern area whose summits are presently shallower than 1000 m, and Stingray Shoal is almost at present sea level. Consequently, it appears that volcanism was intermittent throughout the entire length of the West Mariana Ridge, but with an overall younging to the south. The lack of age information on the individual volcanoes precludes any further speculation about this observation.

The third aspect related to processes that have been active in the West Mariana Ridge is the occurrence of entrenched thalwegs in several of the channels. The channels with pronounced thalwegs are broad and sediment filled with deeply incised thalwegs that wander down the course of a channel until the channel reaches either some low threshold in slope gradient or exits the sediment fill. Not all of the sediment-filled channels have identifiable thalwegs, and thalwegs are not confined to one section of the mapped area. However, the presence of broad sediment-filled channels with incised thalwegs suggests at least two episodes of several stages of channel evolution for these channel systems: episode 1—stage 1 with the initial channel formation, episode 1—stage 2 with the channel filling with a relatively thick sediment sequence, and then episode 2—stage 1 with the re-incision of the channel thalweg. The present stage of the various channel's evolution may represent the latest of several episodes. Regardless of which episode the channel evolution is in, the presence of entrenched thalwegs suggests some change in the channel equilibrium profile has been initiated by uplift of the crest of the West Mariana Ridge, a dropdown of the base of the sediment apron, or perhaps both.

The shallow water depths of many of the volcano summits and the presence of entrenched thalwegs both suggest a postvolcanic stage of uplift of the West Mariana Ridge. The multi-stage nature of the channels, the recent-looking morphology of the erosional channel margins, the unfilled entrenched thalwegs, and the lack of

pelagic sediment within the channels all suggest the channels have been very recently active or are active today. It then follows that the equilibrium profiles of the West Mariana Ridge channels have been disrupted either by uplift on the eastern side, by depression of the western side, or by both. The age-depth profile for the Philippine Sea plate (Park et al., 1990) suggests the plate reached its maximum subsidence perhaps 10 m.y. ago. However, the shallow depths of many of the West Mariana Ridge crest volcanoes suggest significant uplift may have occurred on the eastern edge of the plate long after the Ridge is thought to have become dormant. If this area of the Philippine Sea plate has been volcanically dormant and passively subsiding for the past 10 m.y., and, because almost all of the volcanoes of the West Mariana Ridge are submarine volcanoes (i.e., peaked summits and not guyots), then the crest of the Ridge should be in water depths of at least 1150 m. However, the summits of 33 of the volcanoes on West Mariana Ridge are less than 1150 m deep. Consequently, it seems probable that there has been recent renewed tectonic activity along the eastern crest of the West Mariana Ridge since the volcanism ceased.

The apparent age progression of the volcanoes from oldest in the north and younging to the south suggests volcanism has not been uniform. Perhaps the cross chains reflect flexure of the distal end of the Philippine Sea plate that propagated from north to south. Alternately, perhaps the backarc spreading of the Mariana Trough was not spatially uniform, but rather propagated from north to south.

## CONCLUSIONS

High-resolution (100-m/sounding), multi-beam bathymetry mapping of the western flank of the West Mariana Ridge and adjoining distal region of the Parece Vela Basin suggests the Ridge may not have been dormant for the past 7 m.y. The summits of the Ridge and cross-

chain volcanoes are overwhelmingly peaked in shape and only two of them are guyots. All of the volcanoes are shallower than would be predicted from the subsidence curve for the Philippine Sea plate. If the volcanoes were once subaerial, then there should be many more guyots, if the plate followed the published subsidence curve (Park et al., 1990). If the peaked volcanoes are submarine in origin, then their summits should be much deeper than they are, again using the subsidence curve for the Philippine Sea plate. These observations suggest there may have been significant uplift of the West Mariana Ridge since it is thought to have become dormant ~7 Ma.

Geomorphological evidence suggests a younging of the volcanism of both the West Mariana Ridge and the cross-chain volcanoes. The volcanoes in the north of the Ridge show considerably more erosion on their flanks than do those in the south. However, the southward younging appears not to have been monotonic, but rather volcanism was spatially scattered along the Ridge with a general younging to the south.

A series of canyon-channel systems trend from the crest of the West Mariana Ridge toward the west and onto the proximal Parece Vela Basin. Each system is composed of a second- or third-order dendritic canyon system in the head region and evolves into a large, slightly sinuous channel downstream. Many of the channels have thalwegs entrenched into sediment fill, suggesting a multiphase evolution. High-resolution CHIRP profiles across the channels show that the channel floors lack any pelagic fill, whereas the seafloor adjacent to the channels is capped by pelagic sediment. A large coalesced sediment apron has buried the western flank of the West Mariana Ridge, and this apron has been incised by many of the channel systems. These observations suggest the channel systems have either been recently, or are presently, active and certainly are either contemporaneous with, or postdate, the sediment apron.

## ACKNOWLEDGMENTS

I thank Bob Stern, Patty Fryer, Joel Johnson, Larry Mayer, and Dave Monahan for discussions about the West Mariana Ridge. I especially want to thank Bob Stern for his careful, thoughtful, and detailed review of an earlier version of the manuscript. All of the above provided constructive comments that sharpened my thoughts and my writing, but I take sole credit for any conclusions they might disagree with. I also thank the U.S. Naval Oceanographic Office (NAVO) shipboard staff, especially Mr. Gordon Marsh, the shipboard Senior NAVO Representative, for all their support and generosity during the cruises. This work was funded by National Oceanic and Atmospheric Administration grant NA05NOS4001153 in support of bathymetry mapping for the U.S. Law of the Sea efforts. The data from this mapping, together with images, are available at [http://ccom.unh.edu/law\\_of\\_the\\_sea.html](http://ccom.unh.edu/law_of_the_sea.html).

## REFERENCES CITED

- Anderson, R.N., 1975, Heat flow in the Mariana marginal basin: *Journal of Geophysical Research*, v. 80, p. 4043–4048, doi: 10.1029/JB080i029p04043.
- Babonneau, N., Savoye, B., Cremer, M., and Klein, B., 2002, Morphology and architecture of the present canyon and channel system of the Zaire deep-sea fan: *Marine and Petroleum Geology*, v. 19, p. 445–467, doi: 10.1016/S0264-8172(02)00009-0.
- Clark, J.D., Kenyon, N.H., and Pickering, K.T., 1992, Quantitative analysis of the geometry of submarine channels: Implications for the classification of submarine fans: *Geology*, v. 20, p. 633–638, doi: 10.1130/0091-7613(1992)020<0633:QAOTGO>2.3.CO;2.
- Embley, R.W., Chadwick, W.W., Stern, R.J., Merle, S.G., Bloomer, S.H., Nakamura, K., and Tamura, Y., 2006, A synthesis of multibeam bathymetry and backscatter, and sidescan sonar of the Mariana submarine magmatic arc, western Pacific: *Eos (Transactions, American Geophysical Union)*, Fall Meeting Supplement, Abstract V41B-1723.
- Fisher, A.G., and Heezen, B.C., et al., 1971, Initial Reports of the Deep Sea Drilling Project: Washington, D.C., U.S. Government Printing Office, v. 6, 1329 p.
- Flood, R.D., and Damuth, J.E., 1987, Quantitative characteristics of sinuous distributary channels on the Amazon deep-sea fan: *Geological Society of America Bulletin*, v. 98, p. 728–738, doi: 10.1130/0016-7606(1987)98<728:QCOSDC>2.0.CO;2.
- Fonseca, L., and Calder, B.R., 2005, Geocoder: An efficient backscatter map constructor: U.S. Hydrographic Conference Proceedings (CD-ROM).
- Fonseca, L., and Mayer, L., 2007, Remote estimation of surficial seafloor properties through the application Angular Range Analysis to multibeam sonar data: *Marine Geophysical Researches*, v. 28, p. 119–126, doi: 10.1007/s11001-007-9019-4.
- Fryer, P., 1995, Geology of the Mariana Trough, in Taylor, B., ed., *Backarc basins: Tectonics and Magmatism*: Plenum Press, New York, NY, p. 237–279.
- Fryer, P., 1996, Evolution of the Mariana convergent plate margin system: *Reviews of Geophysics*, v. 34, p. 89–125, doi: 10.1029/95RG03476.
- Fryer, P., Gill, J.B., and Jackson, M.C., 1997, Volcanologic and tectonic evolution of the Kasuga seamounts, northern Mariana Trough: Alvin submersible investigations: *Journal of Volcanology and Geothermal Research*, v. 79, p. 277–311, doi: 10.1016/S0377-0273(97)00013-9.
- Gardner, J.V., 2006b, U.S. Law of the Sea cruise to map the western insular margin and 2500-m isobath of Guam and the Northern Mariana Islands, Cruise BD06-1: University of New Hampshire CCOM-JHC Technical Report 06-100, 37 p., <http://ccom.unh.edu/unclos/report.htm#y2006>.
- Gardner, J.V., 2008, U.S. Law of the Sea cruise to map the western insular margin and 2500-m isobath of Guam and the Northern Mariana Islands, cruise BD07-1: University of New Hampshire CCOM-JHC Technical Report 08-100, 44 p., <http://ccom.unh.edu/unclos/reports.htm#y2008>.
- Gardner, J.V., Mayer, L., and Armstrong, A., 2006a, Mapping supports potential submission to U.N. Law of the Sea: *Eos (Transactions, American Geophysical Union)*, v. 87, p. 157–160, doi: 10.1029/2006EO160002.
- Horton, R.E., 1945, Erosional development of streams and their drainage basins: Hydrophysical approach to quantitative morphology: *Geological Society of America Bulletin*, v. 56, p. 275–370, doi: 10.1130/0016-7606(1945)56[275:EDOSAT]2.0.CO;2.
- Hussong, D.M., and Uyeda, S., 1981, Tectonic processes and the history of the Mariana arc: A synthesis of the results of Deep Sea Drilling leg 60, in Hussong, D., and Uyeda, S., et al., *Initial Reports of the Deep Sea Drilling Project*: Washington, D.C., U.S. Government Printing Office, v. 60, p. 909–929.
- Ishizuka, O., Uto, K., Yuasa, M., and Hochstaedter, A.G., 1998, K-Ar ages from seamount chains in the backarc region of the Izu-Ogasawara arc: *The Island Arc*, v. 7, p. 408–421.
- Jordan, T.H., Menard, H.W., and Smith, D.K., 1983, Density and size distribution of seamounts in the eastern Pacific inferred from wide-beam sounding data: *Journal of Geophysical Research*, v. 88, p. 10,508–10,518, doi: 10.1029/JB088iB12p10508.
- Karig, D.E., 1971, Structural history of the Mariana island arc system: *Geological Society of America Bulletin*, v. 82, p. 323–344, doi: 10.1130/0016-7606(1971)82[323:SHOTMI]2.0.CO;2.
- Karig, D.E., 1972, Remnant arcs: *Geological Society of America Bulletin*, v. 83, p. 1057–1068, doi: 10.1130/0016-7606(1972)83[1057:RA]2.0.CO;2.
- Karig, D.E., and Glassley, W.E., 1970, Dacite and related sediment from the West Mariana Ridge, Philippine Sea: *Geological Society of America Bulletin*, v. 81, p. 2143–2146, doi: 10.1130/0016-7606(1970)81[2143:DARSFT]2.0.CO;2.
- Kirchner, J.W., 1993, Statistical inevitability of Horton's laws and the apparent randomness of stream channel networks: *Geology*, v. 21, p. 591–594, doi: 10.1130/0091-7613(1993)021<0591:SIOHSL>2.3.CO;2.
- Klaus, A., and Taylor, B., 1991, Submarine canyon development in the Izu-Bonin forearc: A seamount II and seismic survey of Aoga Shima Canyon: *Marine Geophysical Researches*, v. 13, p. 131–152.
- Kolla, V., Posamentier, H.W., and Wood, L.J., 2007, Deepwater and fluvial sinuous channels—Characteristics, similarities and dissimilarities, and modes of formation: *Marine and Petroleum Geology*, v. 24, p. 388–405, doi: 10.1016/j.marpetgeo.2007.01.007.
- Kronke, L., and Scott, R., et al., 1981, Initial Reports of the Deep Sea Drilling Program: Washington, D.C., U.S. Government Printing Office, v. 59, 815 p.
- Leopold, L.B., Wolman, M.G., and Miller, J.P., 1964, *Fluvial Processes in Geomorphology*: San Francisco, W.H. Freeman and Company, 522 p.
- Martinez, F., and Fryer, P., 1995, Evolution of back-arc rifting: Mariana Trough, 20°–24°N: *Journal of Geophysical Research*, v. 100, p. 3807–3827, doi: 10.1029/94JB02466.
- Masek, J.G., and Turcotte, D.L., 1994, Statistical inevitability of Horton's laws and the apparent randomness of stream channel networks. Comment and Reply: *Geology*, v. 22, p. 380–381, doi: 10.1130/0091-7613(1994)022<0380:SIOHSL>2.3.CO;2.
- Park, C.-H., Tamaki, K., and Kobayashi, K., 1990, Age-depth correlation of the Philippine Sea back-arc basins and other marginal basins in the world: *Tectonophysics*, v. 181, p. 351–371, doi: 10.1016/0040-1951(90)90028-7.
- Primez, C., and Flood, R.D., 1995, Morphology and structure of Amazon Channel, in Flood, R.D., Piper, D.J.W., and Klaus, A., eds.: *Proceedings of the Ocean Drilling Program, Initial Reports*, v. 155, p. 23–45.
- Smith, W.H.F., and Sandwell, D.T., 1997, Global seafloor topography from satellite altimetry and ship depth soundings: Evidence for stochastic reheating of the oceanic lithosphere: *Science*, v. 277, p. 1956–1962, doi: 10.1126/science.277.5334.1956.
- Smith, W.H.F., and Sandwell, D.T., 2004, Conventional bathymetry, bathymetry from space, and geodetic altimetry: Washington, D.C., *Oceanography*, v. 17, p. 8–23.
- Stern, R.J., and Smoot, N.C., 1998, A bathymetric overview of the Mariana forearc: *The Island Arc*, v. 7, p. 525–540.
- Stern, R.J., Fouch, M.J., and Klemperer, S.L., 2003, An overview of the Izu-Bonin-Mariana subduction factory, in Eiler, J., ed., *Inside the Subduction Factory*: Washington, D.C., *Geophysical Monograph 138*, American Geophysical Union, p. 175–222.
- Strahler, A.H., 1952, Hypsometric (area-altitude) analysis of erosional topography: *Geological Society of America Bulletin*, v. 63, p. 1117–1142, doi: 10.1130/0016-7606(1952)63[1117:HAAOET]2.0.CO;2.
- Troutman, B.M., and Karlinger, M.R., 1994, Statistical inevitability of Horton's laws and the apparent randomness of stream channel networks: Comment and Reply: *Geology*, v. 22, p. 573–575, doi: 10.1130/0091-7613(1994)022<0573:SIOHSL>2.3.CO;2.
- von Huene, R., and Arthur, M.A., 1982, Sedimentation across the Japan Trench off Northern Honshu Island, in Leggett, J.K., ed., *Trench-Forearc Geology: The Geological Society of London, Special Publication 10*, p. 27–47.

MANUSCRIPT RECEIVED 12 AUGUST 2009  
 REVISED MANUSCRIPT RECEIVED 19 JANUARY 2010  
 MANUSCRIPT ACCEPTED 20 JANUARY 2010

Printed in the USA